

# Measurement of SEA parameters for vehicle glasses

M.-H. Moulet<sup>1</sup>, S. Vergne<sup>2</sup>, F. Vanherpe<sup>2</sup>, E. Portier<sup>1</sup>, F. Dupuy<sup>2</sup>,

1: Centre de Transfert de Technologie du Mans, 20 rue Thalès de Milet, F-72000 Le Mans

2: PSA Peugeot Citroën, Centre Technique de Vélizy, Route de Gisy, F-78140 Vélizy Villacoublay

**Abstract:** Statistical Energy Analysis (SEA) models are usually used to estimate the distribution of vibrational energy in a structure build-up of separate parts such as automobiles. In the present paper, different measurement techniques are defined and applied to characterise SEA parameters of car windows. The damping loss factor is measured with the Power Injection Method: the influence of the number of excitations is presented for two windows. A second parameter is studied: the radiation coupling loss factor. Different experimental techniques are used: microphones and intensity probe to measure the acoustic power and accelerometers and intensity probe to measure the space average mean square velocity. Advantages and drawbacks of these techniques are studied.

**Keywords:** SEA parameters, damping loss factors, radiation coupling loss factor, experimental techniques

## 1. Introduction

Statistical Energy Analysis (SEA) models are usually used to estimate the distribution of vibrational energy in a structure build-up of separate parts such as automobiles. The method consists in separating the studied system into mechanically weakly coupled subsystems. In these models, the coupling between subsystems is described by coupling loss factors while internal losses of energy are described by damping loss factors. In the case of a vibrating structure coupled to an acoustic cavity, it is the radiation coupling loss factor that has to be determined.

The aim of this paper is to compare different measurement techniques used to estimate damping loss factors and radiation coupling loss factors in the case of a car window. To measure the damping loss factor, the power input method is chosen: this method is based on a comparison of the dissipated energy of a system to its maximum strain energy under steady state vibration. To calculate the radiation coupling loss factor, it is necessary to measure the radiated power and the structure energy. On these purposes, different measurement techniques are compared (intensity probes, microphones, accelerometers).

In the first part of the paper, definitions of the damping loss factor and the radiation coupling loss factor are reminded. The experimental techniques

used are given in the second part. Then, results for the damping loss factor are presented and the effect of the number of excitations is studied. Finally, results obtained with the different techniques used to measure the radiation coupling loss factor are compared and discussed.

## 2. Damping loss factor

### 2.1 Definition

The damping loss factor used to describe structural damping can be defined as [1]:

$$\eta_{DLF} = \frac{\Delta E}{E_{pot}}, \quad (1)$$

where  $\Delta E$  is the energy dissipated from damping and  $E_{pot}$  is the strain energy.

### 2.2 Power Input Method (PIM)

Assuming a stationary force excitation at one point of the structure,  $\Delta E$  can be replaced with the input energy  $E_{in}$  because the input energy must be equal to the dissipated energy under steady state conditions. Even if the input energy  $E_{in}$  cannot be measured directly, it can be computed from simultaneous measurement of force and velocity at the excitation point as:

$$E_{in}(\omega) = \frac{1}{2\omega} \text{Re}[h_{ff}(\omega)] S_f(\omega), \quad (2)$$

where  $h_{ff}(\omega)$  is the point mobility spectrum at the excitation point and  $S_f(\omega)$  is the power spectral density of the excitation force.

The estimation of the denominator of (1) requires three approximations which are explained in [1]:

- Replacement of the strain energy by the kinetic energy
- Evaluation of the kinetic energy with a reduced number of measurements
- Assumption of a linear system.

With these three approximations, the damping loss factor is calculated using:

$$\eta_{DLF}(\omega) = \frac{\text{Re}[h_{ff}(\omega)]}{\omega \sum_{i=1}^N m_i |h_{ff}(\omega)|^2}, \quad (3)$$

where  $N$  is the number of measurement locations,  $m_i$  is the mass of the discrete portion of the system and  $h_{if}(\omega)$  is the transfer mobility spectrum between the excitation and  $i$  points.

### 2.3 Experimental set-up

For each window,  $N$  accelerometers are glued on the window inside the car (Figure 1(a)). The window is excited by an impact hammer at the accelerometers locations outside the car (Figure 1(b)). Accelerations data are integrated to obtain the different mobilities.

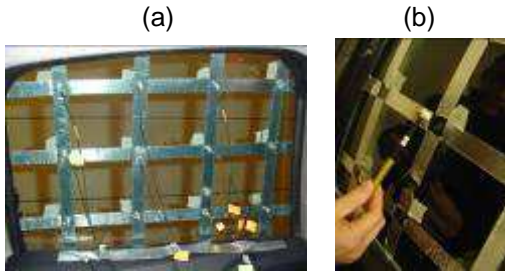


Figure 1: (a) Positions of accelerometers for one car window; (b) Excitation with an impact hammer

### 3. Radiation coupling loss factor

#### 3.1 Definition

For a car window of area  $S_{window}$ , the radiation coupling loss factor is defined as [2]:

$$\eta_{rad} = \frac{\rho_{air} c_{air} \sigma(\omega)}{\omega \rho_{window} e_{window}}, \quad (4)$$

where  $\rho_{air}$  is the air density,  $c_{air}$  is the sound velocity in the air,  $\rho_{window}$  is the material density of the window,  $e_{window}$  is the thickness of the window, and  $\sigma$  is the radiation efficiency which is written:

$$\sigma(\omega) = \frac{P(\omega)}{\rho_{air} c_{air} S_{window} \langle v^2(\omega) \rangle}. \quad (5)$$

In this expression,  $P(\omega)$  is the acoustic power radiated by the car window to the car interior and  $\langle v^2(\omega) \rangle$  is the space average mean square normal velocity of the window.

Finally, the radiation coupling loss factor can be written:

$$\eta_{rad} = \frac{P(\omega)}{\omega \rho_{window} e_{window} S_{window} \langle v^2(\omega) \rangle} \quad (6)$$

#### 3.2 Measurement of acoustic power

To measure the acoustic power  $P(\omega)$ , two methods are proposed. For both of them, the car is placed in a reverberant room. Each part of the structure is acoustically treated except the studied window

(Figure 2) in order to measure the energy coming from this window only. The window is excited by the diffuse field of the reverberant room: the excitation signal is a white noise.



Figure 2: Car in the reverberant room of CTTM

The first method consists in measuring acoustic pressures inside the car interior at eight positions. Then assuming free field conditions inside the car, the radiated power is written:

$$P(\omega) = \frac{1}{\rho_{air} c_{air}} \sum_i \langle p_i^2 \rangle A_i \quad (7)$$

where  $A_i$  is the equivalent absorption area for each microphone  $i$ . These coefficients are calculated from measurements of the reverberation time inside the car. This method is usually used even if the assumption of free field conditions may not be valid.

In the second method, an intensity probe scans the whole window to measure acoustic intensity coming through it.

#### 3.3 Measurement of the space average mean square velocity $\langle v^2(\omega) \rangle$

Two methods are used to measure  $\langle v^2(\omega) \rangle$ . In the first one, accelerations are measured on the surface of the window by an array of accelerometers glued on the interior side (Figure 1(a)). Accelerations are then integrated and averaged to give  $\langle v^2(\omega) \rangle$ .

The second method consists in calculating the space-average mean square normal velocity from scanning data of the intensity probe using [3]:

$$\langle v^2 \rangle = \left( \frac{1}{\rho_{air} \omega d} \right)^2 \frac{[(G_{\rho_1 \rho_1} - G_{\rho_2 \rho_2})^2 + 4(\text{Im}\{G_{\rho_1 \rho_2}\})^2]}{(G_{\rho_1 \rho_1} + G_{\rho_2 \rho_2} + 2\text{Re}\{G_{\rho_1 \rho_2}\})}, \quad (8)$$

where  $d$  is the distance between the two microphones of the probe ( $d=12\text{cm}$ ),  $G_{\rho_i \rho_i}$  is the auto-spectrum of pressure measured by the microphone  $i$ , and  $G_{\rho_1 \rho_2}$  is the cross spectrum of the two pressure signals.

Because of the distance between the two microphones of the intensity probe, the studied frequency bandwidth is [400 Hz-5 kHz].

#### 4. Results for the damping loss factor

##### 4.1 Results for a side window

The damping loss factor is given in Figure 3 for a side window. Results are given in third octave bands. Twelve excitation and response points are used for this window.

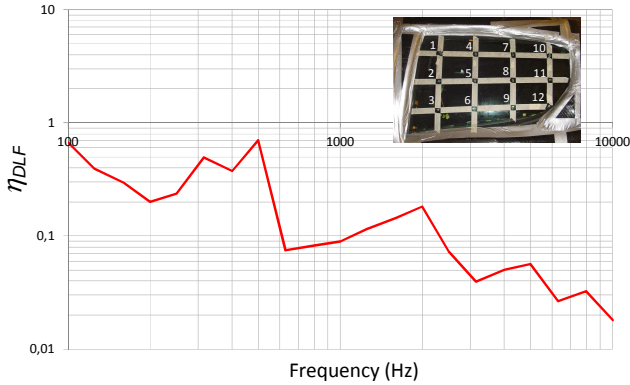


Figure 3: Damping loss factor for a side window

Damping loss factor values are decreasing from 0.7 to 0.02 for the frequency band [500-10000Hz]. These values are higher than the ones usually obtained for tempered glass (smaller than 0.1) [4]. This difference may be explained by the fact that the window is measured with its joints. In order to conclude, we would need a comparison with a FE model or an analytical model.

##### 4.2 Results for the rear window

The damping loss factor is given in Figure 4 for the rear window. Fifteen excitation and response points are used for this window.

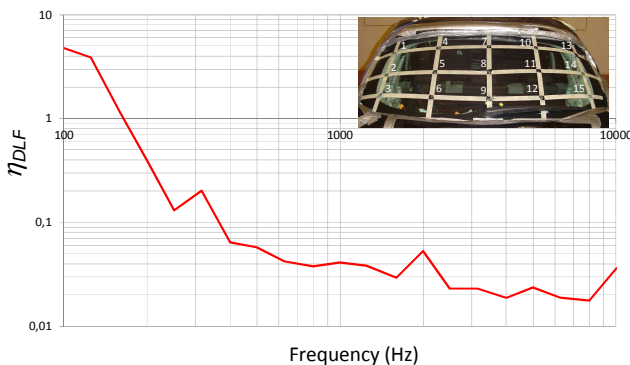


Figure 4: Damping loss factor for the rear window

Damping loss factor values are decreasing from 0.2 to 0.02 for the frequency band [300-10000Hz]. For this window, values are of the same order of magnitude than the ones usually obtained [4].

##### 4.3 Effect of the number of excitations

Different numbers of excitations are used. The number of responses remains the same.

For the side window (Figure 5), we can notice that if the excitation is applied only on even number points or odd number points, results are similar to the ones obtained with twelve excitations. It can be explained by the fact that in both cases, excitation points are distributed on the whole window even if there are less of them. On the contrary, if excitation is applied for points 1 to 6 or for points 7 to 12, there are discrepancies compared with the twelve excitations curve.

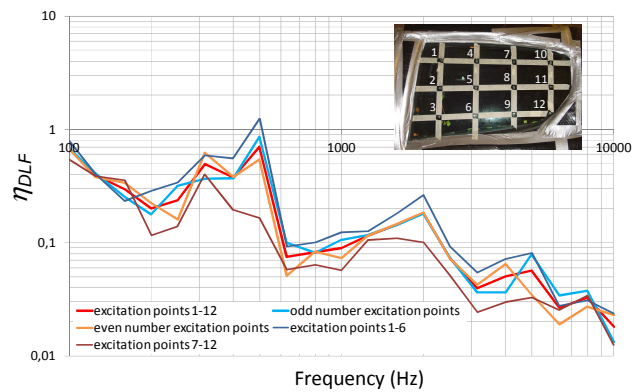


Figure 5: Damping loss factor for a side window: comparison of the number of excitations

For the rear window (Figure 6), the different configurations of excitation give similar results. This can be explained by the symmetry of the rear window: Whether the excitations are localised on the left part or on the right part, the same structural modes are excited and results are similar.

Thus, for symmetric or asymmetric windows, it is possible to reduce the number of excitations: for asymmetric windows, excitations have to be distributed on the whole window while for symmetric windows, excitations can be concentrated on only half of the window (the left or the right part in the case of the rear window for instance).

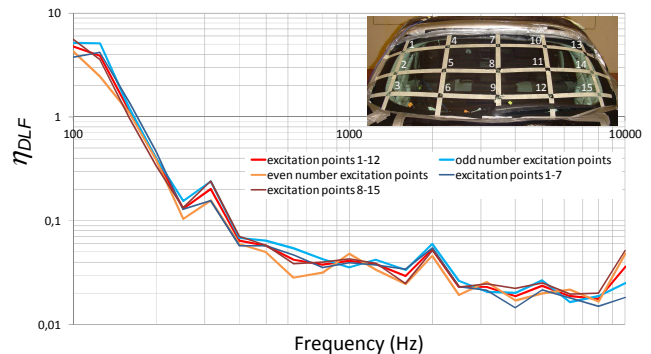


Figure 6: Damping loss factor for the rear window: comparison of the number of excitations

## 5. Results for the radiating coupling loss factor

### 5.1 Preliminary: analytical formulation for the radiation efficiency

The radiation efficiency  $\sigma$  of a finite plate with small damping is given by [5]:

$$\left\{ \begin{array}{ll} \sigma \approx \frac{p c_{air}}{\pi^2 S f_c} \sqrt{\frac{f}{f_c}} & \text{if } f < f_c, \\ \sigma \approx 0.45 \sqrt{\frac{p f_c}{c_{plate}}} & \text{if } f = f_c, \\ \sigma \approx 1 & \text{if } f > f_c \end{array} \right. \quad (9)$$

where  $p$  is the perimeter of the plate,  $S$  the area of the plate,  $c_{plate}$  the sound velocity in the plate and  $f_c$  the coincidence frequency of the plate. Using this expression, it is easy to calculate the radiation coupling loss factor using Eq. (4). In the following, experimental results are compared with analytical ones even if the shape of the window is not taken into account in this model.

### 5.2 Results for a side window

The radiation coupling loss factor is given in Figure 7 for a side window. Results are given in third octave bands.

First, results obtained with the measurement of acoustic power by microphones and the measurement of  $\langle v^2(\omega) \rangle$  by accelerometers (green curve) is in average 50 times higher than the model results.

On the contrary, radiation coupling loss factors obtained from the measurement of power by intensity probe (blue and yellow curves) are of the same order of magnitude than the model results.

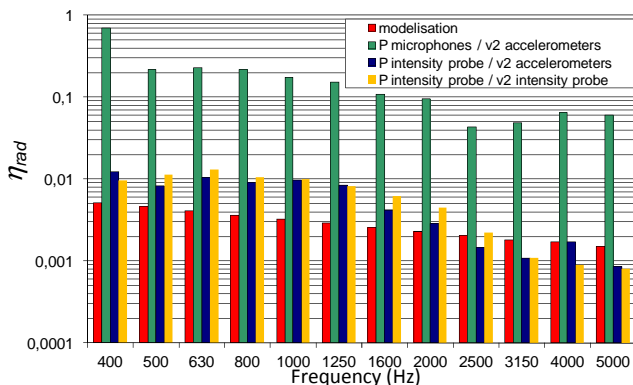


Figure 7: Radiation coupling loss factor for a side window

This high difference can be explained by the big discrepancy between the acoustic power measured by the microphones and the intensity probe (Figure

8). As supposed, the assumption of free field conditions is not valid inside the car .

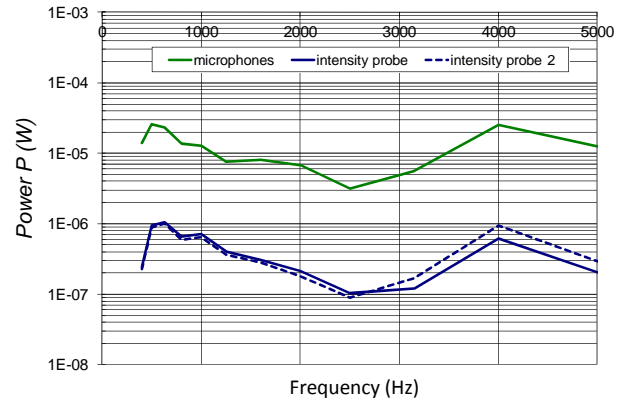


Figure 8: Acoustic power for a side window

About measurement of the space average mean square velocity  $\langle v^2(\omega) \rangle$  (Figure 9), the two methods (accelerometers and intensity probe) give the same kind of result for the side window. This induces similar results for the radiation coupling loss factor (Figure 7).

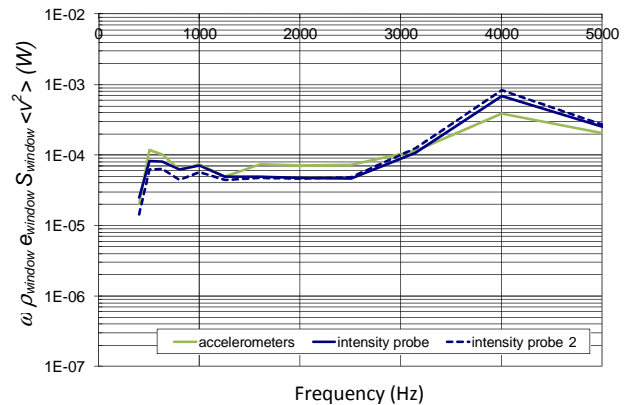


Figure 9: Vibration state measured by accelerometers and intensity probe for a side window

### 5.3 Results for the windscreen

The radiation coupling loss factor is given in Figure 10 for the windscreen.

As for the side window, results obtained with the measurement of acoustic power by microphones and the measurement of  $\langle v^2(\omega) \rangle$  by accelerometers (green curve) is in average 25 times higher than the model results. On the contrary, radiation coupling loss factors obtained from the measurement of power by intensity probe (blue and yellow curves) are of the same order of magnitude than the model results.

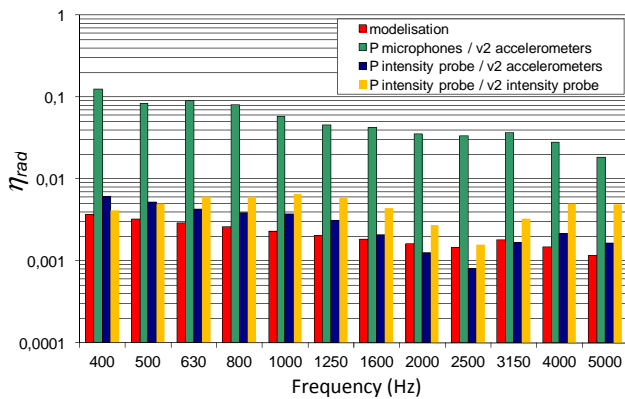


Figure 10: Radiation coupling loss factor for the windscreen

Once more, acoustic power is not well evaluated with the microphone method (Figure 11). However, the use of the intensity probe is not easy for the windscreen: absorbent material must be put on the dashboard in order to avoid reflection. Moreover, acoustic power is measured only for the half superior part of the windscreen because of accessibility problem.

This accessibility difficulty also explains the difference between the space average mean square velocity measured with accelerometers and the one measured with the intensity probe (Figure 12). The probe measurement area is limited to the half superior part of the windscreen while accelerometers are glued on the whole surface. We can nevertheless notice a good repeatability of the measurement with the intensity probe (curves named intensity probe and intensity probe2).

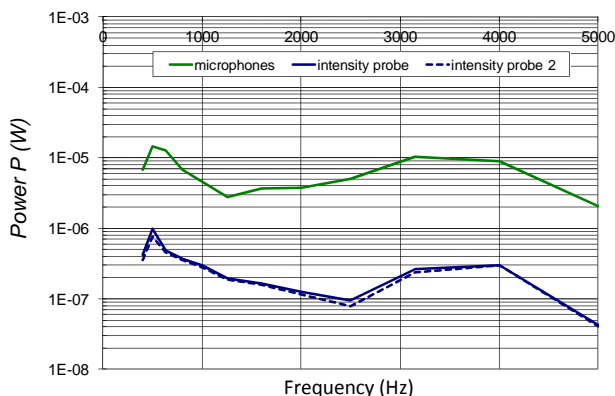


Figure 11: Acoustic power for the windscreen

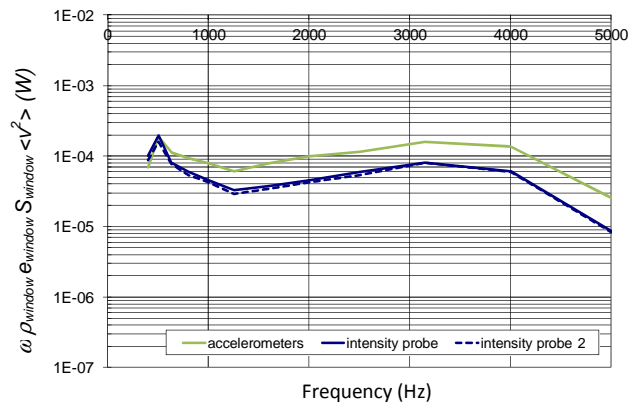


Figure 12: Vibration state measured by accelerometers and intensity probe for the windscreen

## 6. Conclusion

The Power Injection Method allows us to measure damping loss factors that are in the case of the rear window of the same order of magnitude than the one usually found. For the side window, the measured values seem to be overestimated. The dissipation effect of the window's seals may explain this high value. It has been showed that the number of excitation points could be limited as long as they are distributed on the whole window. Next investigation could focus on the limitation of the number of responses.

About the radiating coupling loss factor estimation, the method in which microphones are used to measure the acoustic power inside the car is not suitable: free field conditions assumption is not valid and the acoustic power is overestimated. The radiating coupling loss factor is well estimated with the use of an intensity probe. One advantage of this method is that it allows to measure the acoustic power and the space average mean square velocity of the window in only one scanning. One drawback is that the measurement of acoustic power is sensitive to the reflection inside the car: thus, absorbent material has to be placed on some parts of the car. Moreover the use of the intensity probe requires some space near the studied structure in order to allow scanning. In order to avoid this problem, excitation and response sides could be inverted: a shaker installed inside the car could excite the window while the acoustic power and the velocity of the window could be measured by the intensity probe outside the car in an anechoic room.

## 7. References

- [1] M. Carfagni, M. Pierini, "*Determining the Loss Factor by the Power Input Method (PIM), Part 1: Numerical Investigation*", Journal of Vibration and Acoustics, Vol. 121, July 1999, pp. 417-421.
- [2] L. Gagliardini, D. Thenail, G. Borello: "*Virtual SEA for noise prediction and structure borne sound modelling*", Rieter Automotive Conference, Pfaffikon, Switzerland, June 14-15, 2007.
- [3] F. J. Fahy: "*Sound Intensity*", Chapter 10, p. 236. E&FN Spon, an Imprint of Chapman & Hall, 1995.
- [4] B. Bloss, M. Rao, "*Measurement of Damping in Structures by the Power Input Method*", Experimental Techniques, Vol. 26, No. 3, May/June 2002, pp. 30-32.
- [5] L. Cremer, M. Heckl, "*Structure-Borne Sound: Structural Vibrations and Sound Radiation at Audio Frequencies*", 2nd ed.; translated and revised by E.E. Ungar., Springer-Verlag Berlin, 1988